

Pairing dynamics in particle transport

Guillaume Scamps* and Denis Lacroix†

GANIL, CEA/DSM and CNRS/IN2P3, Boîte Postale 55027, 14076 Caen Cedex, France

G.F. Bertsch‡

*Institute for Nuclear Theory and Department of Physics,
University of Washington, Seattle, Washington 98195, USA*

Kouhei Washiyama§

*Physique Nucléaire Théorique, CP229, Université Libre de Bruxelles, B-1050 Bruxelles, Belgium and
GANIL, CEA/DSM and CNRS/IN2P3, Boîte Postale 55027, 14076 Caen Cedex, France*

We analyze the effect of pairing on particle transport in time-dependent theories based on the Hartree-Fock-Bogoliubov (HFB) or BCS approximations. The equations of motion for the HFB density matrices are unique and the theory respects the usual conservation laws defined by commutators of the conserved quantity with the Hamiltonian. In contrast, the theories based on the BCS approximation are more problematic. In the usual formulation of TDHF+BCS, the equation of continuity is violated and one sees unphysical oscillations in particle densities. This can be ameliorated by freezing the occupation numbers during the evolution in TDHF+BCS, but there are other problems with the BCS that make it doubtful for reaction dynamics. We also compare different numerical implementations of the time-dependent HFB equations. The equations of motion for the U and V Bogoliubov transformations are not unique, but it appears that the usual formulation is also the most efficient. Finally, we compare the time-dependent HFB solutions with numerically exact solutions of the two-particle Schrödinger equation. Depending on the treatment of the initial state, the HFB dynamics produces a particle emission rate at short times similar to that of the Schrödinger equation. At long times, the total particle emission can be quite different, due to inherent mean-field approximation of the HFB theory.

PACS numbers:

Keywords:

I. INTRODUCTION

Pairing is essential to the global description of nuclear ground-state and low excited state properties; the Hartree-Fock-Bogoliubov (HFB) and Hartree-Fock augmented by BCS (HF+BCS) theories are in common use to treat the pairing degrees of freedom [1]. Also in nuclear reactions, many phenomena are expected to be influenced by pairing correlations: collective motion, fusion, fission, transfer reactions and nuclear break-up. The obvious candidate theory to treat these effects is the Time-Dependent Hartree-Fock Bogoliubov (TDHFB) theory [2], and there has been much effort in the last decade to apply it. However, the TDHFB theory turns out to be much more complicated to implement than the corresponding time-dependent Hartree-Fock theory, and the applications have been mainly performed in its small amplitude limit, the Quasi-particle RPA (QRPA) [3–10]. However, most of the phenomena quoted above are far from small amplitude excursions from the ground state, and transport theories able to treat Large Am-

plitude Collective Motion (LACM) are mandatory. Recently, several groups have applied the TDHFB [11–13] to nuclear dynamics. An approximate version of theory, called TDHF+BCS, has also been considered [14]. We will discuss its properties as well. Most recent applications have been to small-amplitude collective motion in nuclei, where the theory is equivalent to the quasiparticle random-phase approximation (QRPA). Still, it is important to understand and solve the theory here as a first step towards treating large-amplitude motion.

The aim of the present article is first to present from a rather general point of view different dynamical theories that incorporate pairing correlations. We find that the TDHFB has many good properties, but it is difficult to find further simplifying approximations. We find that the TDHF+BCS approximation leads to a break-down of the continuity equation. This failure might induce serious difficulties in the description of physical processes. The second aim of the paper is to test various implementations of the pair theory in a model problem. For this purpose, we examine a one-dimensional model of particle evaporation for which we also have a numerical exact solution.

*Electronic address: scamps@ganil.fr

†Electronic address: lacroix@ganil.fr

‡Electronic address: bertsch@uw.edu

§Electronic address: kouhei.washiyama@ulb.ac.be

II. FORMALISM

The TDHFB theory and the TDHF+BCS approximations have been recently applied to nuclear physics in Ref. [11–14]. In this section we will briefly summarize the main features.

A. The TDHFB theory

The main equations of TDHFB theory, Eq. (5-6) below, can be derived in at least two different ways. One way is from the general variational principle,

$$S = \int_{t_i}^{t_f} \langle \Psi(t) | i\hbar \partial_t - H | \Psi(t) \rangle dt, \quad (1)$$

see e.g. Ref. [15]. Here H denotes the Hamiltonian and $|\Psi\rangle$ is a HFB wave function. The equations may also be derived by demanding that the operators for the ordinary and anomalous densities, $\hat{\rho}_{ij} = a_j^\dagger a_i$ and $\hat{\kappa}_{ij} = a_j a_i$ respectively, satisfy Ehrenfest's theorem:

$$i\hbar \partial_t \langle \Psi | a_j^\dagger a_i | \Psi \rangle = \langle \Psi | [a_j^\dagger a_i, H] | \Psi \rangle, \quad (2)$$

$$i\hbar \partial_t \langle \Psi | a_j a_i | \Psi \rangle = \langle \Psi | [a_j a_i, H] | \Psi \rangle. \quad (3)$$

In the following, we will further assume that H is a two-body hamiltonian,

$$H = \sum_{ij} h_{ij}^0 a_i^\dagger a_j + \frac{1}{4} \sum_{ijkl} \bar{v}_{ijkl} a_i^\dagger a_j^\dagger a_l a_k. \quad (4)$$

where \bar{v} denotes the anti-symmetric two-body matrix elements. The derived TDHFB equations are:

$$i\hbar \frac{d}{dt} \rho = h\rho - \rho h + \kappa \Delta^* - \Delta \kappa^*, \quad (5)$$

$$i\hbar \frac{d}{dt} \kappa = h\kappa + \kappa h^* + \Delta(1 - \rho^*) - \rho \Delta. \quad (6)$$

Here ρ , κ , h and Δ are all matrices of dimension equal to that of the single-particle space. The matrices h and Δ are the mean-field and pairing field of the Hamiltonian, defined as

$$h_{ij} = h_{ij}^0 + \sum_{kl} \bar{v}_{iljk} \rho_{kl}, \quad \Delta_{ij} = \frac{1}{2} \sum_{kl} \bar{v}_{ijkl} \kappa_{kl}. \quad (7)$$

The dynamical equation can be recast in a more compact form by introducing the generalized density matrix \mathcal{R} and generalized single-particle hamiltonian \mathcal{H} :

$$\mathcal{R} = \begin{pmatrix} \rho & \kappa \\ -\kappa^* & 1 - \rho^* \end{pmatrix}, \quad \mathcal{H} = \begin{pmatrix} h & \Delta \\ -\Delta^* & -h^* \end{pmatrix}. \quad (8)$$

With these definitions the equation of motion becomes [15, Eq. 9.61a]

$$i\hbar \frac{d}{dt} \mathcal{R} = [\mathcal{H}, \mathcal{R}]. \quad (9)$$

This generalizes the usual TDHF picture by replacing the one-body density by \mathcal{R} . Similarly to the TDHF case, the generalized density satisfies $\mathcal{R}^2 = \mathcal{R}$ and has only eigenvalues equal to zero and one [15, 16].

Going back to ordinary Hartree-Fock theory, it is computationally advantageous to factorize the density matrix and express it as a sum over the contributions from occupied orbitals to obtain equations of motion for the individual orbitals. There is no obvious advantage for the factorization in TDHFB because all of the single-particle orbitals in Fock space contribute to the generalized density matrix \mathcal{R} . Nevertheless, the factorization is usually applied to obtain the actual equations to be solved numerically. To write equations in this form, one needs an explicit form of the Bogoliubov transformation,

$$\beta_\alpha = \sum_i U_{i\alpha}^* a_i + V_{i\alpha}^* a_i^\dagger. \quad (10)$$

The density matrices are expressed as $\rho = V^* V^T$ and $\kappa = V^* U^T$, and the generalized density matrix is

$$\mathcal{R} = \begin{pmatrix} V^* \\ U^* \end{pmatrix} \begin{pmatrix} V^T & U^T \end{pmatrix}. \quad (11)$$

One can then easily see that Eq. (9) will be satisfied if we require the $\{U, V\}$ matrix be a solution of

$$i\hbar \frac{d}{dt} \begin{pmatrix} U \\ V \end{pmatrix} = \begin{pmatrix} h & \Delta \\ -\Delta^* & -h^* \end{pmatrix} \begin{pmatrix} U \\ V \end{pmatrix}. \quad (12)$$

The numerical solution of the TDHFB equations are usually carried out in this representation [12, 13]. However, it should be remembered that there are redundant variables in the $\{U, V\}$ representation corresponding to unitary transformations of the quasiparticle basis, and in fact Eqs. (12) are not unique.

We may derive another form of the TDHFB equations as follows. The wave function $|\Psi\rangle$ at any time t is the quasi-particle vacuum associated with the Bogoliubov transformation that transforms the physical vacuum to $|\Psi(t)\rangle$. In that representation, the Hamiltonian has zero-, two-, and four-quasiparticle terms that can act on $|\Psi(t)\rangle$ [16]. Neglecting the four-quasiparticle excitation amplitudes, the result is

$$\begin{aligned} H|\Psi(t)\rangle &\simeq H'(t)|\Psi(t)\rangle \\ &= \left[\langle H \rangle + \frac{1}{2} \sum_{\alpha\beta} H_{\alpha\beta}^{20} \beta_\alpha^\dagger(t) \beta_\beta^\dagger(t) \right] |\Psi(t)\rangle \end{aligned} \quad (13)$$

with [16, Eq. (E.22)]

$$H^{20} = U^\dagger h V^* - V^\dagger h^T U^* + U^\dagger \Delta U^* - V^\dagger \Delta^* V^* \quad (14)$$

According to the Thouless theorem, any state of the form $(1 + \sum_{\alpha\beta} Z_{\alpha\beta} \beta_\alpha^\dagger \beta_\beta^\dagger) |\Psi\rangle$ can be expressed as a new quasiparticle vacuum [16]. To lowest order in Z , the Bogoliubov transformation to the new vacuum from the physical vacuum is given by

$$\begin{pmatrix} U' & V'^* \end{pmatrix} = \begin{pmatrix} U & V^* \end{pmatrix} \begin{pmatrix} 1 & Z^* \\ Z^* & 1 \end{pmatrix} \quad (15)$$

We can thus derive an equation of motion by demanding that the changes in U, V just match the two quasiparticle excitations generated by H . After a lengthy but straightforward derivation, it may be shown that the corresponding equations of motion for U and V can be written as:

$$\begin{cases} i\hbar\partial_t U = \rho h^\dagger U - \kappa h^* V \\ \quad - \kappa \Delta^* U + \rho \Delta V \\ i\hbar\partial_t V = -(1 - \rho^*) h^* V - \kappa^* h^\dagger U \\ \quad - \kappa^* \Delta V - (1 - \rho^*) \Delta^* U \end{cases} \quad (16)$$

These equations differ from (12) but nevertheless lead to the same TDHFB equation for the generalized density.

B. The TDHF+BCS approximation

The TDHF+BCS treatment of pairing dynamics is motivated by the simple form the wave function has in the BCS approximation,

$$|\Psi\rangle = \prod_{k>0} (u_k + v_k a_k^\dagger a_{\bar{k}}^\dagger) | \rangle. \quad (17)$$

The TDHF+BCS approximation may be derived from a variational principle [17] or by an approximate reduction of the TDHFB equations [14]. For the reduction of the TDHFB equations, we first note that wave function can be put into BCS form at any fixed time by transforming the U, V matrices to the canonical basis. In that basis, ρ is diagonal and κ matrix is zero except for one element on each row (or column) representing the pair $i\bar{i}$. Assuming that the Δ matrix has the same structure as κ , Ref. [14] shows that the TDHFB time evolution preserves the same canonical structure with orbitals that evolve by the mean field Hamiltonian,

$$i\hbar\partial_t |\varphi_k\rangle = h |\varphi_k\rangle. \quad (18)$$

where h has been defined in Eq. (7). The equations of motion for ρ and κ in this time-dependent basis are¹

$$i\hbar \frac{d}{dt} n_k = \Delta_k \kappa_k^* - \Delta_k^* \kappa_k, \quad (19)$$

$$i\hbar \frac{d}{dt} \kappa_k = +\Delta_k (1 - 2n_k). \quad (20)$$

Here n_k , κ_k and Δ_k are short-hand notations for ρ_{kk} , $\kappa_{k\bar{k}}$ and $\Delta_{k\bar{k}}$ respectively.

One technical point should be mentioned. When Eq. (18) is integrated, there is an irrelevant phase factor $\exp(-i \int^t \langle \varphi_k(t') | h_{HF}(t') | \varphi_k(t') \rangle dt')$ introduced into the

time-dependent orbitals. For computational reasons the phase is removed by integrating

$$i\hbar\partial_t |\varphi_k\rangle = (h[\rho] - \eta_k) |\varphi_k\rangle \quad (21)$$

instead of Eq. (18), with $\eta_k(t) = \langle \varphi_k(t) | h_{HF} | \varphi_k(t) \rangle$. At the same time, Eq. (20) is replaced by

$$i\hbar \frac{d}{dt} \kappa_k = \kappa_k (\eta_k + \eta_{\bar{k}}) + \Delta_k (1 - 2n_k). \quad (22)$$

Finally, we mention that the TDHF+BCS approximation was found to work well with a separable pairing interaction and in the small amplitude limit [14].

C. Conservation laws and equation of continuity

Since the TDHFB density matrix satisfies Ehrenfest's theorem, it is trivial to show that the conservation laws for one-body observables are respected by the TDHFB dynamics. It was also shown that conservation laws for important observables such as particle number are satisfied in TDHF-BCS [14]. However, for transport we are interested in local conservation laws as well. In particular, if the interaction is local the coordinate-space density $n(x, t)$ should satisfy the equation of continuity,

$$\frac{dn(x, t)}{dt} = -\vec{\nabla} \cdot \vec{j}(x, t) \quad (23)$$

where $\vec{j}(x)$ is the particle current. Assuming a local interaction, Eq. (23) may be derived from Ehrenfest's theorem, evaluating the commutator on the right hand side as

$$\vec{\nabla} \cdot \vec{j}(x) = \langle [\hat{n}(x), H] \rangle = -\frac{\hbar^2}{2m} \langle [\hat{n}(x), \nabla^2] \rangle. \quad (24)$$

This is sufficient to guarantee that TDHFB obeys the equation of continuity under the stated condition. Unfortunately, this is not true for the TDHF+BCS dynamics.

Within TDHF+BCS, the local density is given by

$$n(x, t) = \sum_i n_i(t) |\varphi_i(x, t)|^2, \quad (25)$$

and its evolution satisfies

$$\begin{aligned} \frac{dn(x, t)}{dt} &= \sum_i n_i (\varphi_i^*(x, t) \partial_t \varphi_i(x, t) + \varphi_i(x, t) \partial_t \varphi_i^*(x, t)) \\ &+ \sum_i |\varphi_i(x, t)|^2 \partial_t n_i(t) \end{aligned} \quad (26)$$

The first terms on the left are just the evolution of the orbitals under a mean-field potential, and so the same reduction applies as in Eq. (23). The result is

$$\frac{dn(x, t)}{dt} = -\vec{\nabla} \cdot \vec{j}(x, t) + \sum_i |\varphi_i(x, t)|^2 \left(\frac{dn_i(t)}{dt} \right) \quad (27)$$

Thus continuity cannot be guaranteed unless the occupation numbers are fixed. We will see below that TDHF+BCS can produce unphysical density oscillations when the occupations are allowed to vary.

¹ Note that these equations slightly differ from those from [14], due to the definition of κ_k here.

III. APPLICATION TO PARTICLE EVAPORATION

Recently two of us (DL and KW) began investigating the effect of pairing on particle evaporation, and obtained the results shown in Fig. 1. Skipping over the details, the number of particles escaping an initially excited nucleus is shown as a function of time using either the 3D-TDHF code of Ref. [18–20] or an upgraded version including pairing using the TDHF+BCS theory proposed in Refs. [14, 17]. As we can see, the standard mean-field calculation presents the expected long time decay due to particle evaporation[21]. When pairing is included, the number of particles in the nucleus first decays and then starts to oscillate. Clearly, this result is unphysical. It was this unphysical result that motivated us to undertake the present more general study. For the present article, we consider a more simplified Hamiltonian that permits us to compare a number of approximations with each other and with a numerically exact solution. In the present article, we investigate whether the observed problem is systematic in theories where pairing is included or if it comes from the specific treatment of pairing in the TDHF+BCS approximation using zero range interaction. Our study is also the occasion to benchmark different theories, TDHF+BCS and TDHFB, to describe particle emission.

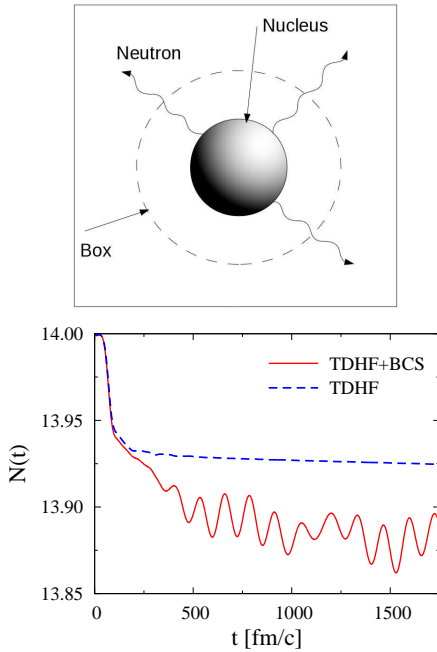


FIG. 1: Top: Schematic illustration of neutron evaporation from a nucleus of O^{22} excited by a monopole boost at $t=0$. Bottom: Number of neutron inside a sphere of size 10 fm around the nucleus as a function of time obtained with TDHF and TDHF+BCS (from [22]).

A. A one-dimensional model

For comparing the different treatments of pairing dynamics, we consider a one-dimensional system composed of N particles in a box with x in the range $-X_{\max} < x < X_{\max}$ and a Hamiltonian of the form

$$H = \sum_i^N \left\{ \frac{p_i^2}{2m} + U(x_i) \right\} + \sum_{i < j}^{N(N-1)/2} v(x_i - x_j) [1 - P_{\sigma_i \sigma_j}]. \quad (28)$$

Here, $P_{\sigma_i \sigma_j}$ denotes the spin-exchange operator. The potential $U(x)$ is taken to be a Woods-Saxon well centered at the origin:

$$U(x) = \frac{U_0}{1 + \exp[(|x| - X_0)/a]}. \quad (29)$$

The two-body interaction $v(x - x')$ is taken to be a finite-range Gaussian

$$v(x - x') = v_0 \exp\left(-\frac{(x - x')^2}{2\sigma_0^2}\right) \quad (30)$$

In the limit where the range σ_0 goes zero, $v(x - x')$ is a contact interaction and our model is similar to the model considered in Ref. [23] to analyse the onset of vortices in rotating Fermi gas using TDHFB. The advantage of a finite range is that it does not have to be renormalized for use in BCS or HFB.

The TDHFB is formulated in a Fock space and the space has finite dimension in numerical implementations. Our particle creation and annihilation operators $\psi_\sigma^\dagger, \psi_\sigma$ are defined on a uniform mesh of points $\{x\}$ with spacing Δx ; $\sigma = \uparrow$ or \downarrow is the spin label. Then we can write the quasiparticle transformation as [23]

$$\beta_\alpha^\dagger = \Delta x \sum_x \left(u_\alpha(x, t) \psi_\uparrow^\dagger(x) + v_\alpha(x, t) \psi_\downarrow(x) \right). \quad (31)$$

$$\beta_{\alpha'}^\dagger = \Delta x \sum_x \left(u_{\alpha'}(x, t) \psi_\downarrow^\dagger(x) + v_{\alpha'}(x, t) \psi_\uparrow(x) \right). \quad (32)$$

In the following, we will use the convention $\Delta x \sum_x \rightarrow \sum_x$ and not distinguish between the quasiparticle sets α and α' , with the property $u_{\alpha'}(x, t) = u_\alpha(x, t)$ and $v_{\alpha'}(x, t) = -v_\alpha(x, t)$. The discretized time-dependent equations in version Eq. (12) of TDHFB take the explicit form

$$i\hbar \frac{\partial}{\partial t} u_\alpha(x, t) = \left\{ -\frac{\hbar^2 \Delta_x^2}{2m(\Delta x)^2} + U(x) + \Gamma(x) \right\} u_\alpha(x, t) - \sum_{x'} \Delta(x, x') v_\alpha(x', t) \quad (33)$$

and

$$i\hbar \frac{\partial}{\partial t} v_\alpha(x, t) = - \left\{ -\frac{\hbar^2 \Delta_x^2}{2m(\Delta x)^2} + U(x) + \Gamma^*(x) \right\} v_\alpha(x, t)$$

$$-\sum_{x'} \Delta^*(x, x') u_\alpha(x', t). \quad (34)$$

with

$$\Gamma(x) = \sum_{x'} v(x - x') \rho(x', x'), \quad (35)$$

$$\Delta(x, x') = v(x - x') \kappa(x, x'). \quad (36)$$

Here $\Delta_x^{(2)}$ is the second-difference operator, $\Delta^{(2)}\phi(i) = \phi(i+1) - 2\phi(i) + \phi(i-1)$.

The normal and anomalous density matrix are given by

$$\rho(x, x) = \sum_{\alpha} |v_\alpha(x, t)|^2 \quad (37)$$

$$\kappa(x, x') = \sum_{\alpha} v_\alpha^*(x) u_\alpha(x'). \quad (38)$$

B. Exact solution for the two particle case

One interesting aspect of the model considered here is that for two particles it can be solved exactly numerically. Indeed, assuming that the system is a spin singlet, the two-body wave-function reads:

$$\Phi(x_1, \sigma_1, x_2, \sigma_2) = \frac{1}{\sqrt{2}} (\delta_{\sigma_1 \uparrow} \delta_{\sigma_2 \downarrow} - \delta_{\sigma_1 \downarrow} \delta_{\sigma_2 \uparrow}) \phi(x_1, x_2) \quad (39)$$

where $\phi(x_1, x_2)$ is a symmetric function that satisfies the Schrödinger equation:

$$i\hbar \frac{d}{dt} \phi(x_1, x_2) = [h_1^0 + h_2^0 + v(x_1 - x_2)] \phi(x_1, x_2), \quad (40)$$

Since the discussion here might be applied not only to nuclear systems but also to other field of physics like condensed matter or atomic physics, we consider here reduced units. The length, time-scale and energy scale given below are respectively written in units of Δx , $m\Delta x^2/\hbar$ and $\hbar^2/(m\Delta x^2)$ where Δx is the discretization mesh step. Accordingly, all quantities below will be presented without specific units. The parameters of the central potential are set to $a = 2$, $X_0 = 4.5$ and $\sigma_0 = 2.5$ and the initial harmonic constraint is taken as $\lambda = 6.173 \times 10^{-4}$. Three interaction strength v_0 equal to -1.096×10^{-2} , -3.344×10^{-2} , and -6.280×10^{-2} are considered. The three cases will be referred respectively to case (a), (b) and (c) below. In each case, the depth of the Woods-Saxon potential has been adjusted to get the same binding energy $E = -2.2 \times 10^{-2}$, leading to $U_0 = -2.7 \times 10^{-2}$, -1.929×10^{-2} and -7.716×10^{-3} respectively. For cases (a) and (b) the interaction is below the strength needed for a condensate in the HFB or BCS theory at a mean particle number of two.

An illustration of the two-body density matrix obtained in different level of approximation for the case (a) are shown in Fig. 2. Due to the attractive nature

of the two-body interaction used, the two-body density presents a clear correlation along the axis $(x_1 + x_2)/2$ that is completely neglected at the Hartree-Fock level. Such a correlation is partially recovered when pairing is included in the HFB or BCS theory.

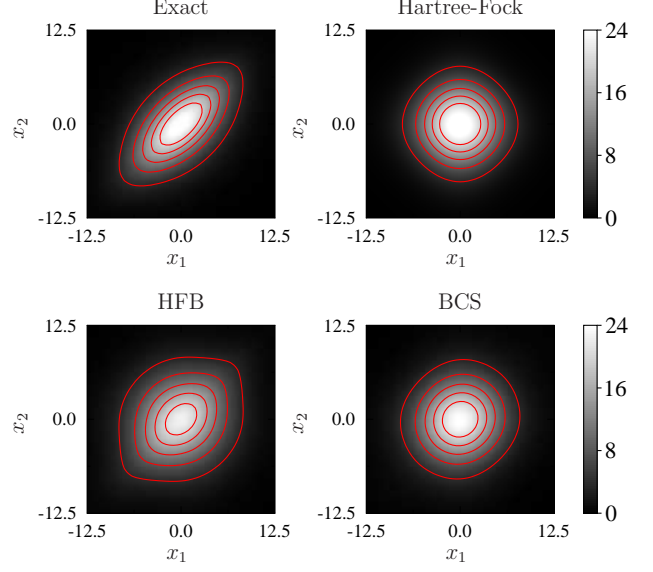


FIG. 2: $S = 0$ component of the two body density matrix $\rho^{(2)}(x_1 \uparrow, x_2 \downarrow)$ in 10^{-3} (unit of length) $^{-2}$ at time $t = 0$ for the four theories studied here. This figure correspond to the set of parameters (c) (see text).

C. Some numerical aspects for dynamics with pairing

It is important to integrate the time-dependent equations of motion with a high-order method, because wave function conditions such as normalization and conserved quantities such as energy can be easily lost. The time scale for single-particle motion and direct reactions is several thousand of units of time, and we require numerical accuracy up to those times. For most of the results we present below, we have used the fourth-order Runge-Kutta algorithm (RK4). The calculations in Ref. [13] on the other hand use a sixth-order Adam-Bashford algorithm, and we have tested that as well.

Typically, we take a box of dimension $X_{max} = 500$, giving the HFB matrices a dimension of $4X_{max}/\Delta x = 2000$. The single-particle Hamiltonian has a range up to ~ 2 , which requires a fairly small time step. We take $\Delta t = 0.263$.

1. Ehrenfest vs Thouless equation of motion

As has been stressed in section II A, the equation of motion on the (u_α, v_α) components are not unique. We

have implemented two of the formulations below, namely the “Ehrenfest” (Eq. (12)) and the “Thouless” (Eq. (16)) equations of motion. The numerical integration can be carried out very accurately using each version of the equations. We found that the Thouless equation has a better precision than the Ehrenfest equation using RK4 at a fixed time step. However, it turns out that the Ehrenfest formulation is three or four times faster than the Thouless one, due to the smaller number of matrix operation in Eqs. (12) compared to Eqs. (16). Since the computational time is a crucial aspect of the numerical treatment, the standard Ehrenfest equation is a better choice. The density formulation (Eq. (5-6)) would have a similar number of matrix operations to the Thouless formulation, but we have not investigated the numerical performance of this third alternative.

2. Imaginary absorbing potential

Particle loss is monitored by computing the number of particles having $|x| < X_0/2$. Particles can be reflected from the edges of the box and obscure this measure of evaporation, so we have to add an absorbing potential h_i near the edges. As mentioned in Ref. [12], the specific form of the absorbing potential is not obvious, because it should decrease the particle number without affecting the normalization of the wave function. It can be shown that the following prescription satisfies these requirements,

$$i\hbar \frac{\partial}{\partial t} \begin{pmatrix} u \\ v \end{pmatrix} = \begin{pmatrix} h - \rho h_i & -\Delta - \kappa h_i \\ -\Delta^* + \kappa^* h_i & -h^* + (1 - \rho^*) h_i \end{pmatrix} \begin{pmatrix} u \\ v \end{pmatrix}.$$

In particular, the above equation preserves the unitarity property $uu^\dagger + v^*v^t = 1$.

In applications below, the imaginary potential is taken as

$$h_i(x) = 0 \quad \text{for } |x| < (X_{\max} - x_{im}),$$

$$h_i(x) = iV_{im} \frac{|x| - X_{\max} + x_{im}}{x_{im}} \quad \text{for } |x| > (X_{\max} - x_{im})$$

with $X_{\max} = L_{\max}/2$, $V_{im} = -7.716 \times 10^{-3}$ and $x_{im} = 37.5$.

We have compared TDHFB evolution in small box including the imaginary potential with the corresponding evolution in very large box to check that the present method is a practical way to suppress the reflected particles. We also found that a simpler prescription is also adequate for our purposes. Namely, one can apply the imaginary potential to the v amplitudes alone, with the equation of motion

$$i\hbar \frac{\partial}{\partial t} \begin{pmatrix} u \\ v \end{pmatrix} = \begin{pmatrix} h & -\Delta \\ -\Delta^* & -h^* + h_i \end{pmatrix} \begin{pmatrix} u \\ v \end{pmatrix}.$$

This prescription violates unitarity, but the results using it could not be distinguished from the correct evolution.

D. Particle evaporation

To simulate an evaporating system, we start with a wave function that is constrained to be largely inside the potential well $U(x)$. This is achieved by adding a small harmonic constraining field λr^2 to the Hamiltonian and solving for the HFB ground state. At time $t \geq 0$, the harmonic constraint is removed inducing a monopole oscillation of the system that is eventually damped out by particle evaporation. This is illustrated in Fig. 3, showing snapshots of the density at different times with the system evolved with the TDHF equations of motion, i.e. without pairing.

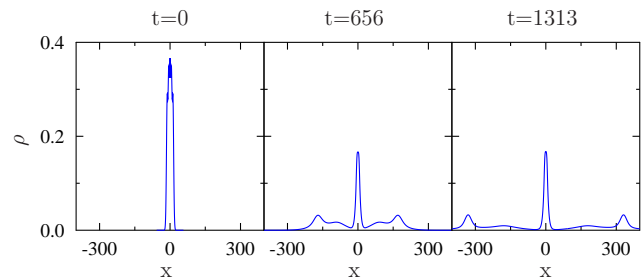


FIG. 3: Evolution of the local one-body density $n(x)$ of a system of $N = 10$ particles. The system is initially confined in a harmonic trap. At $t \geq 0$, the external constrained is relaxed.

1. Comparison between the exact solution and TDHFB

In this section we will compare the particle emission of TDHFB with that given by the two-particle Schrödinger equation, solved numerically. One should not expect close agreement under all conditions for two reasons. The total emission probability in the final state can be calculated easily in the Schrödinger dynamics by taking the overlap of the initial state with the bound solutions. The TDHFB dynamics on the other hand may have no binding when the average particle number on the nucleus becomes small.

It is also not possible to set the initial conditions for the HFB wave function to correspond exactly to the two-particle wave function of the Schrödinger equation; one sees this already in Fig. 2. As described above, the initial state for the Schrödinger equation is squeezed ground state, namely the lowest state of the two-particle system in the presence of a harmonic external potential. A corresponding HFB wave function could be constructed by using the BCS form of the wave function and requiring that it have the same one-particle density matrix. This turns out to not work well, due to high momentum components in the wave function that are not properly controlled by the HFB pairing field. We found that a better prescription is to make a corresponding squeezed ground state in the HFB treatment. We use this prescription for

the comparison shown below.

We measure the number of particles inside the system by the quantity

$$N(t) = \int_{|x| < X_{\text{box}}} 2n(x, t) dx, \quad (41)$$

where X_{box} here is taken as 100. Note that the system is centered at $x = 0$. The evolution of $N(t)$ for several cases is shown in Figure 4, comparing the exact results with the HFB approximation.

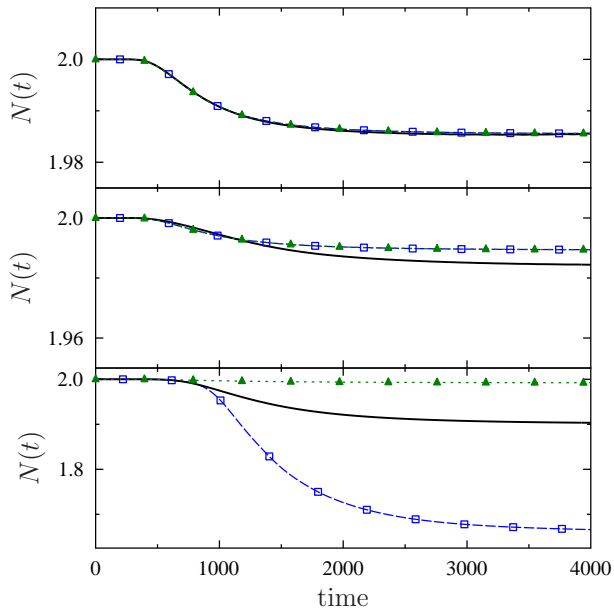


FIG. 4: Number of particles evaporated from an initially compressed system with initially $N = 2$ as a function of time obtained with the exact (solid black line) and TDHF (filled green triangle) and TDHFB (open blue squares). Results with different two-body interaction strengths (case (a), (b) and (c)) are respectively shown from top to bottom (see text).

In the case (a) and (b), TDHF and TDHFB are identical. Indeed, the minimization of HFB equation to get the initial state leads to a pure Slater determinant state. In these case, the TDHF evolution is very close to the exact solution. Note that, in this regime, the evaporation is dominated by the mean-field contribution and pairing has a weak effect on particle emission. As the interaction strength increases, the TDHFB and TDHF results starts to deviate from each other as well as from the exact evolution. As the interaction strength increases, the role of pairing and, more generally, correlations on evaporation becomes more important. The TDHF evolution largely underestimate the emission in case (c). This stems from the fact that mean-field is not able to properly describe the diffusion of the occupation probability around the Fermi energy in the initial state and the dynamical scattering of single-particles during the evolution induced by correlations beyond the Hartree-Fock. In bottom panel of

figure 4, the lack of evaporation in TDHF is due to the fact that all initial occupied states can be decomposed onto bound states of the corresponding mean-field. A similar situation occurs for the $N = 10$ case presented below.

A precise study of the strongest coupling case (case (c)), which is the only case above the HFB threshold for the initial state, shows that the time scale associated to particle evaporation is properly accounted for in TDHFB. This could indeed be seen in bottom part of figure 4 where we see that the time at which $N(t)$ starts to decrease is the same in the exact and in the TDHFB case. This shows that the time-scale associated with the evaporation process is the same in the exact and TDHFB case. In the long time limit, TDHFB overestimates the average number of emitted particles. Accordingly, it could be anticipated that the internal motion of the system is more damped in the latter case than in reality. We indeed have checked that the damping width of the monopole resonance is larger in TDHFB compared to the exact solution.

It should be noted that the approximation leading to TDHFB can only be justified for the short-time evolution. Indeed, even starting from a quasi-particle state, correlation beyond TDHFB might built up in time, like for instance four quasi-particle excitations.

2. Comparison between the exact solution and TDHF+BCS

Here, the results obtained by using the TDHF+BCS equation of motion discussed in section II B are presented. In figure 5, an illustration of the result obtained in the case (c) is shown.

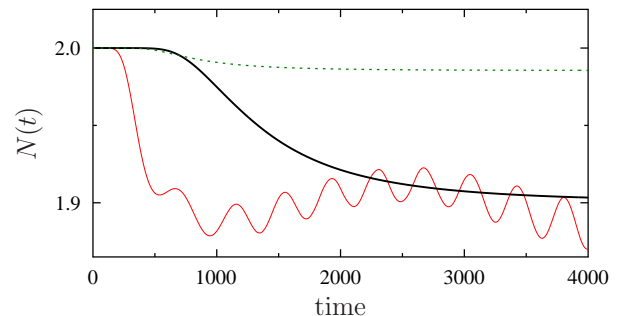


FIG. 5: Number of particles evaporated from an initially compressed system with initially $N = 2$ as a function of time obtained with the exact (solid black line), TDHF (dashed green line) and TDHF+BCS theory (thin red line) in the case of parameter set (c).

Independently of the set of parameters used in the model case, it is generally observed that the TDHF+BCS theory leads to unrealistically fast early emission of particles compared to the exact case. This fast emission seems to be a generic feature of the BCS approach as illustrated in Figs. 6 where $N = 10$ particles are considered.

Independently of the set of parameters used in the model case, it is generally observed that the TDHF+BCS theory leads to unrealistically fast early emission of particles compared to the exact case. This fast emission seems to be a generic feature of the BCS approach as illustrated in Figs. 6 where $N = 10$ particles are considered. This observed fast emission is very likely connected the problem of applying BCS when continuum states are present in the wave functions. The BCS ground state has a unphysical gas of particles in the continuum rather than an exponential decay into the vacuum [24]. This was one of the historical reason why HFB was preferred to BCS in nuclear structure studies. It is of course possible to reduce the continuum problem by truncating the number of single-particle states that contribute to pairing. However, we do not know any systematic way to carry this out without reference to more reliable calculational methods.

In studies dedicated to nuclear structure, this is generally circumvented by reducing significantly the number of single-particle states that contribute to pairing. Then, only states with single-particle energy within a given range ΔE around the Fermi energy are used, where ΔE is of the order of few MeV. In Figures 4-6, this restriction has not been made and a large set of single-particles is retained. If the energy window ΔE is reduced, the time-scale associated to particle evaporation is increased and eventually becomes more consistent with the exact dynamics. Conjointly, the asymptotic number of evaporated particles is significantly reduced and approaches the TDHF case as ΔE goes to zero.

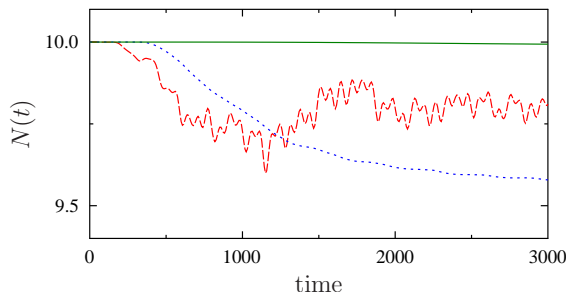


FIG. 6: Number of particles evaporated from an initially compressed system with initially $N = 10$ as a function of time obtained with the TDHF (solid line), TDHFB (dotted line) and TDHF+BCS theory (dashed line).

It should be mentioned that in realistic three-dimensional calculations, there is no flexibility in the selection of single-particle states contributing to the dynamics. Indeed, static calculation are already made with a specific choice of single-particle space in such a way that with an effective force in the pairing channel, the gap has a reasonable value. Accordingly, the dynamics should be made with the same set of single-particles states has is already done in Ref. [14].

3. Spurious oscillation in TDHF+BCS theory

In the long time evolution, oscillation of the number of particles, similar to those displayed in figure 1 are observed in TDHF+BCS, see Figs. 5 and 6. Such oscillations are absent in the TDHFB theory. From the application presented here, we can conclude that the spurious oscillations is a generic effect in TDHF+BCS. It occurs even if a finite range interaction is used. Finally, this problem is solved when TDHFB is used.

To better characterize the oscillation, $N(t)$ can be expressed in the canonical basis as

$$N(t) = \sum_i n_i(t) P_i(t), \quad (42)$$

where $n_i(t)$ and $P_i(t)$ denote respectively the occupation numbers and the probability of the canonical orbital i inside the box:

$$P_i(t) = \int_{|x| \in X_{\text{box}}} |\varphi_i(x, t)|^2 dx. \quad (43)$$

An illustration of $N(t)$ for the two particle case (c) is given in figure 7. The observed evolution is mainly due to the evolution of the two closest levels below and above the particle emission threshold labelled respectively by "1" and "2". These two levels verify $n_1(t) + n_2(t) \simeq 1$. During time evolution, the unbound level is continuously emitted while the bound level remains in the box, i.e. $P_1(t) = 1$. Assuming, that only these two levels contribute to the particle emission, an estimate $N'(t)$ of the number of evaporated particles is given by ²:

$$N'(t) = 2 [n_1(t) P_1(t) + n_2(t) P_2(t)]. \quad (44)$$

The evolution of $n_i(t)$ and $P_i(t)$ for $i = 1, 2$, as well as $N'(t)$ are shown in Fig. 7 attesting for the validity of the two-level approximation. As seen in bottom part of this figure, $N'(t)$ is very close from its exact value $N(t)$ and oscillations are due to oscillations in occupation numbers

Such oscillations of occupation numbers are expected in any theory beyond TDHF, including the TDHFB and/or exact evolution (see Fig. 8). However, these theories do not lead to unphysical evolution of particle number. The difference between TDHF+BCS and the two other theories stems from the approximation made to get the equation of motions. Indeed, by neglecting the off-diagonal matrix elements of the pairing field, the single-particle evolution reduces to self-consistent mean-field dynamics, similar to the TDHF one. The effect of correlation only enters into the occupation numbers evolution, and only affects the single-particle evolution through the density dependence of the self-consistent mean-field.

² Note that the factor 2 here comes from the initial degeneracy

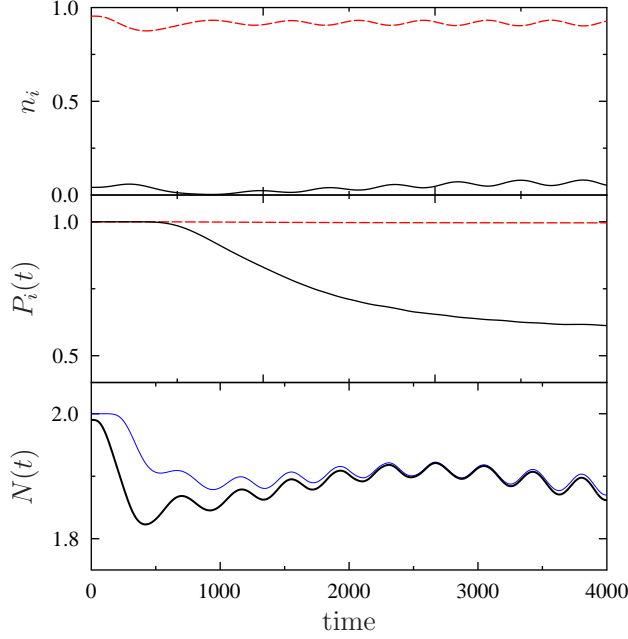


FIG. 7: Top: Evolution of occupation numbers of the two closest states above (state 2, dashed line) and below (state 1, solid line) the Fermi energy as a function of time obtained in TDHF+BCS (parameters set (c)). Middle: Evolution of the corresponding portion of the wave-function remaining inside the box. Bottom: Evolution of $N(t)$ (thin line) and of $N'(t)$ (thick line) as a function of time.

Usually, correlation is expected to induce a mixing of single-particle states. Indeed, the evolution of the one-body density matrix in the presence of correlation is given by:

$$i\hbar \frac{\partial \rho}{\partial t} = [h(\rho), \rho] + Tr_2[v_{12}, C_{12}], \quad (45)$$

where $h(\rho)$ is the mean-field of the correlated state while v_{12} and C_{12} denotes the two-body interaction and correlation matrix respectively (see Ref. [25] for more details). In both TDHFB and exact solution, the second term induces an extra mixing of single-particle states that is neglected in TDHF+BCS. It turns out that this mixing is essential to compensate the possible oscillations in occupation numbers. This is clearly illustrated in Fig. 8 where the quantity $P_i(t)$ are shown to oscillate coherently with $n_i(t)$ in the exact case (similar behavior is observed in TDHFB evolution).

4. Link with the break-down of continuity equation in TDHF+BCS

Starting from the expression (27) derived for TDHF+BCS, the evolution of particle number inside the

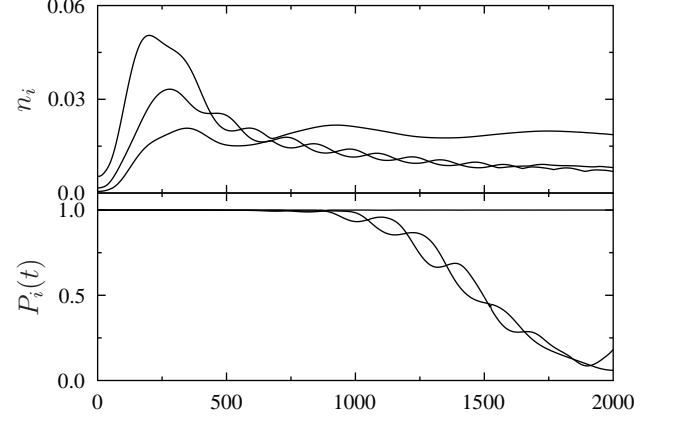


FIG. 8: Top: Evolution of occupation numbers of the three main single-particle canonical states contributing to the particle evaporation for the exact dynamics. The corresponding values of $P_i(t)$ are shown in the bottom part.

box is given by

$$\frac{dN(t)}{dt} = - \int_{|x| \in X_{\text{box}}} \text{div}(j(x, t)) dx + \sum_i P_i(t) \left(\frac{dn_i(t)}{dt} \right). \quad (46)$$

Introducing two sets of real functions $R_i(x, t)$ and $S_i(x, t)$ for each wave-packet such that:

$$\varphi_i(x, t) = R_i(x, t) \exp(iS_i(x, t)/\hbar), \quad (47)$$

and making use of partial integration technique, the first term in eq. (46) can be recast as:

$$\int_{|x| \in X_{\text{box}}} \text{div}(j(x, t)) dx = 2 \sum_i n_i |\varphi_i(X_{\text{box}}, t)|^2 v_i(X_{\text{box}}, t),$$

where v_i denotes the local velocity of the particle defined through $v_i(x, t) \equiv \nabla S_i(x, t)/m$.

This term is the expected physical term expected to appear in any well defined transport theory that relates the number of particles inside the box to the flow of particles outgoing at the boundary of the box. However, due to the presence of the second term in eq. (46), oscillation of occupation numbers that are not compensated by oscillation of the probability $P_i(t)$ (see figure 7) lead to spurious behavior of the particle number. The only way out to avoid this problem in a TDHF+BCS approach is to freeze the occupation numbers during the evolution.

5. TDHF+BCS with frozen occupation numbers

To incorporate pairing in a transport model we are facing the difficulty that the TDHFB theory is very de-

manding numerically. A possible solution to this difficulty, would be to use the simpler TDHF+BCS approach. However, in view of preceding sections, the approximation made to obtain TDHF+BCS leads to unphysical behavior especially when continuum plays a significant role: strange behavior of particle emission, gas problem.

We have seen in section III D 3, that the pathologies of TDHF+BCS comes from the evolution of occupation that should normally be accompanied by a consistent mixing of the single-particle states along the dynamical path. This approximation does not seem to be critical in the study of static properties of nuclei and most often, for not too exotic nuclei, BCS theory provides a fairly good approximation to HFB.

A simple prescription to avoid non-physical evolution in TDHF+BCS is to assume that the occupation numbers are frozen during the time-evolution, this approximation is called hereafter *frozen occupation approximation* (FOA). An illustration of the FOA effect on particle evaporation is shown in figure 9 (dashed line). As anti-

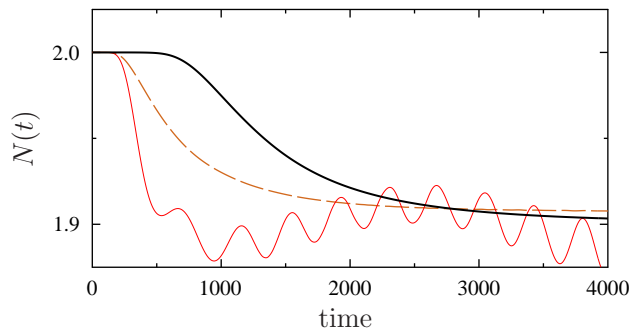


FIG. 9: Evolution of the number of particles evaporated from an initially compressed system of $N = 2$ particles. The exact result (thick solid line) is compared to the TDHF+BCS with (dashed line) and without (thin solid line) the frozen occupation number approximation. The simulation has been made with the same parameters set as the lower panel of figure 4.

pated, spurious oscillations of the particle number evaporation disappear in the FOA. It turns out, that, for the specific set of parameters used in the example of figure 4, the asymptotic number of particle evaporated is in very good agreement with the exact case, much better than the TDHFB solution (see figure 4). However, the agreement depends on the parameters that are used and not systematic conclusion can be drawn. Note that this ap-

proximation has already been used in realistic calculation for example to study dipole giant resonances [26].

IV. SUMMARY

In this article, different transport theories able to incorporate pairing are discussed. One important conclusion is that theories like TDHF+BCS where the continuity equation is not respected can lead to unphysical results. More specifically, the effect of pairing on particle emission has been analyzed here using a simple one-dimensional Hamiltonian that can be solved exactly for the case of two particles. From the systematic study we have made by changing the interaction strength and/or particle number, pairing does affect significantly the particle number emission. While the TDHF approach generally underestimate significantly the number of emitted particles, an enhancement of particle evaporation is observed when pairing is included. This effect is automatically included in both TDHFB or TDHF+BCS theory. Only TDHFB provides a good description of particle emission at short time but might deviates from the exact dynamics at longer time due to accumulated correlation effects beyond this approach.

While the asymptotic number of emitted particles is quite reasonable, TDHF+BCS leads to unphysical rapid emission and spurious oscillations of the number of emitted particles. The direct use of TDHF+BCS, that would be highly desirable from the practical point of view, is plagued with unphysical behavior, and, as we have shown, it is preferable to use a simplified version where occupation numbers are frozen to their initial value.

In summary, both TDHFB and TDHF+BCS with constant occupation numbers can eventually be used to describe a physical system while TDHF+BCS with varying occupation numbers should be avoided. While TDHFB is expected to have a richer dynamics, due to its simplicity, the second transport theory remains quite attractive.

Acknowledgment

GFB thanks A. Bulgac for discussions. We also acknowledge the France-US Institute for Physics of Exotic Nucleus for collaborative support. GFB was also supported by the US Dept. of Energy under Grant DE-FG02-00ER41132.

[1] M. Bender, P.-H. Heenen, P.-G. Reinhard, Rev. Mod. Phys. **75**, 121 (2003).
 [2] C. Simenel, D. Lacroix, and B. Avez, Quantum Many-Body Dynamics: Applications to Nuclear Reactions (VDM Verlag, Sarrebruck, Germany, 2010); posted as arXiv:0806.2714

[3] K. Hagino and H. Sagawa, Nucl. Phys. A **695**, 82 (2001).
 [4] M. Matsuo, Nucl. Phys. A **696** 371 (2001).
 [5] M. Grasso, N. Sandulescu, N. Van Giai, R. J. Liotta, Phys. Rev. C **64**, 064321 (2001).
 [6] E. Khan, N. Sandulescu, N. Van Giai, M. Grasso, Phys. Rev. C **66**, 024309 (2002).

- [7] N. Paar, T. Niksic, D. Vretenar, and P. Ring, Phys. Rev. C **69**, 054303 (2004).
- [8] T. Nakatsukasa and K. Yabana, Eur. Phys. J. A **20**, 163 (2004).
- [9] J. Terasaki and J. Engel, Phys. Rev. C **74**, 044301 (2006).
- [10] S. Péru, G. Gosselin, M. Martini, M. Dupuis, S. Hilaire, and J.-C. Devaux, Phys. Rev. C **83**, 014314 (2011).
- [11] Y. Hashimoto and K. Nodeki, arXiv:0707.3083.
- [12] B. Avez, C. Simenel, and Ph. Chomaz, Phys. Rev. C **78**, 044318 (2008).
- [13] I. Stetcu, A. Bulgac, P. Magierski, K.J. Roche, Phys. Rev. C **84**, 051309(R) (2011)
- [14] S. Ebata, T. Nakatsukasa, T. Inakura, K. Yoshida, Y. Hashimoto, and K. Yabana, Phys. Rev. C **82**, 034306 (2010).
- [15] J.P. Blaizot and G. Ripka, Quantum Theory of Finite Systems, (MIT Press, Cambridge, Massachusetts, 1986).
- [16] P. Ring and P. Schuck, The Nuclear Many-Body Problem, (Springer, 1980).
- [17] J. Blocki and H. Flocard, Nucl. Phys. A **273**, 45 (1976).
- [18] K.-H.Kim, T.Otsuka, and P. Bonche, J. Phys. G **23**, 1267 (1997).
- [19] C. Simenel, Ph. Chomaz, and G. de France, Phys. Rev. Lett. **86**, 2971 (2001).
- [20] K.Washiyama and D. Lacroix, Phys. Rev. C **78**, 024610 (2008).
- [21] N. Van Giai, Ph. Chomaz, P.F. Bortignon, F. Zardi, R.A. Broglia, Nucl. Phys. A **482**, 437 (1988).
- [22] K. Washiyama and D. Lacroix (private communication).
- [23] G. Tonini, F. Werner, and Y. Castin, Eur. Phys. J. D **39**, 283 (2006).
- [24] J. Dobaczewski, H. Flocard, and J. Treiner, Nucl. Phys. A **422**, 103 (1984).
- [25] D. Lacroix, S. Ayik, and Ph. Chomaz, Prog. Part. Nucl. Phys. **52**, (2004) 497.
- [26] J.A. Maruhn et al., Phys. Rev. C **71**, 064328 (2005)